Ichthyol Res
DOI 10.1007/s10228-014-0408-9

FULL PAPER

Phylogeography of Blacktip Grouper, *Epinephelus fasciatus* (Perciformes: Serranidae), and influence of the Kuroshio Current on cryptic lineages and genetic population structure

Kaoru Kuriiwa · Satoru N. Chiba · Hiroyuki Motomura · Keiichi Matsuura

Received: 4 December 2013 / Revised: 6 April 2014 / Accepted: 17 April 2014

Abstract To investigate the influence of the Kuroshio Current on the high diversity of marine fishes in Japanese waters, the intraspecific phylogeographic structure of Blacktip Grouper, *Epinephelus fasciatus,* was determined. The genetic analysis of *E. fasciatus* indicated three intraspecific mtDNA lineages representing different evolutionary histories: the first lineage differentiated in Japanese waters during a long period of fluctuations of the ancient Kuroshio Current, the second lineage, widely distributed in the tropical western Pacific, was transported to Japanese waters by the Kuroshio Current and the third lineage was distributed primarily around the Ogasawara (Bonin) Islands. Present-day sympatric distributions of the three lineages, characterized by different ratios of such individuals at each geographic site, indicated a complex genetic pattern that was classified into three demographic groups, the dispersal and gene flows of which were strongly influenced by the Kuroshio Current and factors such as countercurrent and island arc. Genetic breaks in *E. fasciatus* populations were congruent with other fish faunal boundaries in Japanese waters.

Keywords Marine biogeography · Dispersal · Migration · Pelagic larval duration

Introduction

The Kuroshio Current, one of the world's major ocean currents, flows from east of the Philippines to the Pacific coast of southern mainland Japan, via Taiwan and the southern tip of the Ryukyu Islands. This current transports tropical fishes from the Philippines and Taiwan to Japanese waters resulting in overlapping distributions of tropical and warm temperate fishes in the southern part of the latter region (Nishimura 1992). Senou et al. (2006) indicated that another important role of the current was to create an invisible barrier to temperate fishes when they try to move southward. The Kuroshio Current and cold Oyashio Current (Kuril Current), extending southwards to northern Japan, have resulted in a high diversity of marine organisms in Japanese waters (Fujikura et al. 2010). This diversity has been the subject of frequent biogeographical investigations (e.g., Jordan 1901; Tanaka 1931; Briggs 1974; Nishimura 1992; Nakabo 2002). Although several faunal provinces in Japanese waters were defined on the bases of water temperature and the ocean currents, quantitative faunal data were not considered. In contrast, Senou

Electronic supplementary material The online version of this article (doi:10.1007/s10228-014-0408-9) contains supplementary material, which is available to authorized users.

K. Kuriiwa · S. N. Chiba · K. Matsuura
National Museum of Nature and Science,
4-1-1 Amakubo, Tsukuba, Ibaraki 305-0005, Japan

S. N. Chiba
e-mail: chiba_s@kahaku.go.jp

K. Matsuura
e-mail: matsuura@kahaku.go.jp

Present Address:
K. Kuriiwa (✉)
Faculty of Science, Department of Chemistry, Biology and Marine Science, University of the Ryukyus,
1 Senbaru, Nishihara, Okinawa 903-0213, Japan
e-mail: kaorukuriiwa@07.alumni.u-tokyo.ac.jp

H. Motomura
Kagoshima University Museum, 1-21-30 Korimoto,
Kagoshima 890-0065, Japan
e-mail: motomura@kaum.kagoshima-u.ac.jp

Published online: 27 May 2014

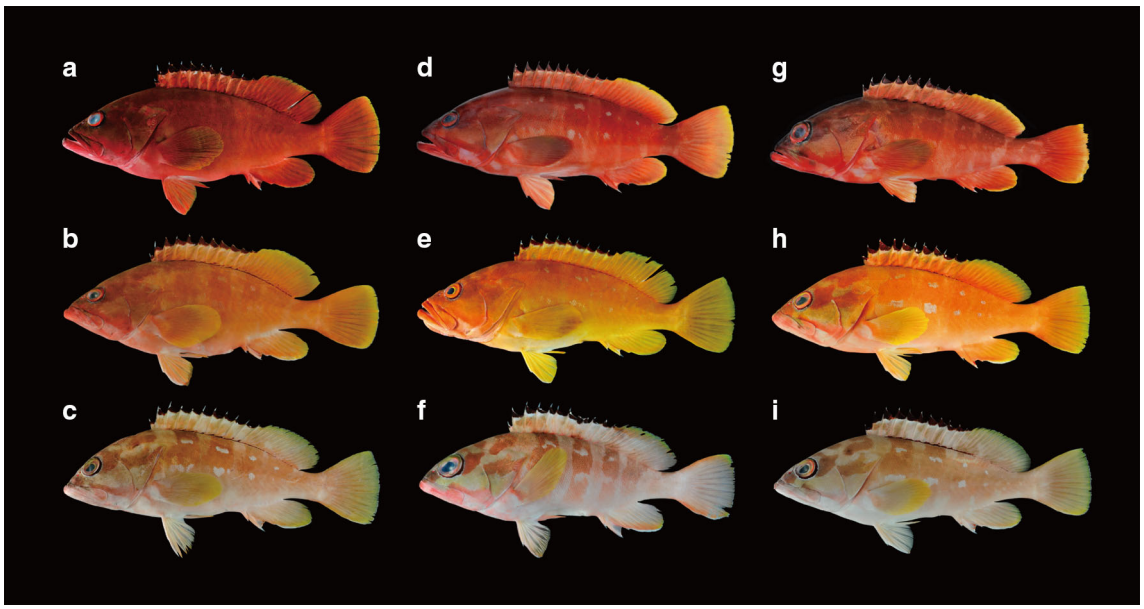

Fig. 1 Color variations of *Epinephelus fasciatus*. **a** Kozu Island (collection locality), NSMT-P 96600 (registration number of voucher specimen), 29.5 cm SL (standard length); **b** Shimokoshiki-jima Island, NSMT-P 95762, 31.4 cm SL; **c** Ogasawara Islands, NSMT-P 95263, 24.6 cm SL; **d** Fukue Island, NSMT-P 91761, 29.0 cm SL; **e** Tanegashima Island, KAUM-I 9069, 33.5 cm SL; **f** Yaeyama Islands, NSMT-P 93854, 15.8 cm SL; **g** Kodakara-jima Island, NSMT-P 91974, 18.1 cm SL; **h** Ogasawara Islands, NSMT-P 93541, 26.0 cm SL; **i** Ogasawara Islands, NSMT-P 95268, 23.2 cm SL

et al. (2006) and Matsuura and Senou (2012) conducted cluster analyses for the marine fish fauna of southern Japan, which indicated two distinct faunal groups. In these faunal analyses, however, the population sizes of fishes in each geographic site were not considered. In addition, although a pair of closely related species distributed in each faunal group was considered, it is unclear whether cryptic genetic breaks in widely distributed species around southern Japan exist. A greater understanding of the fish diversity of these faunal groups requires detailed population or species level biogeographical analyses.

Phylogeography, a relatively recent biogeographical approach, is shedding light on the principles and processes governing the geographic distributions of genealogical lineages, especially those within and among closely related species (Avise 2000). The present study focused on the intraspecific phylogeographic structure of Blacktip Grouper, *Epinephelus fasciatus*, in Japanese waters and the tropical western Pacific so as to determine how the Kuroshio Current may have influenced this fish's evolutionary history. *Epinephelus fasciatus*, one of the most common and widespread species of the genus in the tropical Indo-West Pacific, is also known from subtropical to temperate waters in Japan (Randall and Heemstra 1991). In addition, ecological characteristics of the species have been well documented in aquaculture studies: (1) adult fishes spawn pelagic eggs, (2) pelagic larval duration (PLD) is approximately two months, (3) larval settlement is at approximately 5 cm in total length (TL), (4) upon reaching 20 cm TL, most individuals are reproductively mature, and (5) the species is protogynous, half of the subadult individuals changing sex to become male (Kawabe et al. 1997, 2000; Kawabe 2005; Kawabe and Kohno 2009).

Our observations on *E. fasciatus* in Japanese waters show differences in body coloration (Fig. 1) and maximum body size based on geographic region. Most temperate water individuals reach up to 50 cm TL, including those around the Izu Islands (populations 2–4 in Table 1 and Fig. 2) and the main islands of Japan (5–13). These fishes are characterized by bright red body coloration, whereas those in tropical/subtropical waters around the Ogasawara (Bonin) Islands (1), the Ryukyu Islands (14–21) and further south (22–27), have orange or whitish coloration and reach up to 35 cm TL. Many surveys using the phylogeographic approach revealed that marine fishes generally show a shallower phylogeographic structure than that of freshwater/brackish-water fishes as a result of their continuous habitat and relatively lengthy pelagic larval dispersal (Palumbi 1994; Grant and Bowen 1998; Avise 2000). However, the dual role of the Kuroshio Current and/or some other past events may cause discrete genetic structures in *E. fasciatus* with phenotypic and quantitative variations mentioned above. The phylogeographic structures and evolutionary history of *E. fasciatus* around Japan and adjacent waters are elucidated below.

Table 1 Collection localities, geographic population numbers and number of individuals examined of *Epinephelus fasciatus*

Locality	Geographic population number	Number of individuals examined
Japan, Ogasawara (Bonin) Islands	*1*	60
Izu Islands		
Hachijo-jima Island	*2*	2
Kozu Island	*3*	32
Izu-oshima Island	*4*	31
Main islands of Japan		
Izu Peninsula	*5*	20
Mie Prefecture	*6*	20
Tokushima Prefecture	*7*	2
Kochi Prefecture	*8*	2
Northern part of Miyazaki Pref. (Kadogawa)	*9*	20
Southern part of Miyazaki Pref. (Nangou)	*10*	22
Fukue Island	*11*	20
Kagoshima Prefecture	*12*	1
Shimokoshiki-jima Island	*13*	16
Ryukyu Islands		
Tanegashima Island	*14*	19
Yaku-shima Island	*15*	22
Kuchino-shima Island	*16*	10
Gaja-jima Island	*17*	20
Kodakara-jima Island	*18*	16
Amami-oshima Island	*19*	10
Okinawa Island	*20*	25
Yaeyama Islands	*21*	30
Taiwan, East coast (Su-ao, Hualien, Cheng-gon, and Fugang)	*22*	25
Southern coast (Hengchun)	*23*	20
West coast (Wuchi and Penghu)	*24*	12
Vietnam, Nha Trang	*25*	35
Malaysia, Kota Kinabalu	*26*	26
Indonesia, Bitung (Northern tip of the Sulawesi Island)	*27*	23

Materials and methods

Fish samples. In total, 541 individuals of *Epinephelus fasciatus* were used in this study, comprising specimens from Japan (400), Taiwan (57), Vietnam (35), Malaysia (26) and Indonesia (23) (Fig. 2; Table 1). Thirteen additional species of *Epinephelus* were selected as outgroup species [Electric Supplementary Material (ESM) Table S1], based on phylogenetic analyses and a revised classification of the tribe Epinephelini (Craig and Hastings 2007). Species identification and nomenclature followed Randall and Heemstra (1991) and Senou (2002). Specimens were obtained by spear-fishing, line-fishing or from fish markets between 2007–2011. Voucher specimens were deposited in the National Museum of Nature and Science (NSMT - formerly National Science Museum, Tokyo), the Kagoshima University Museum (KAUM), the Fisheries Research Laboratory, Mie University (FRLM) and Division of Fisheries Sciences, Faculty of Agriculture, Miyazaki University (MUFS). All tissue samples and extracted DNA were deposited in NSMT. Specimen details and DNA data for the fishes used in this study are given in Table S1. The map with submarine topographies was created by the Generic Mapping Tools (GMT) ver. 4.5.7 (University of Hawaii: http://gmt.soest.hawaii.edu/).

DNA extraction, PCR amplification and sequencing. Total genomic DNA was extracted from the tissues using the Gentra® Puregene™ Tissue Kit (QIAGEN), following the manufacturer's protocol. A segment of approximately 2.3 kbp of mitochondrial DNA (mtDNA) was amplified by the polymerase chain reaction (PCR) with a pair of primers. The primer sequences were Epi-cyF: 5'-ATG GCH AGC CTH CGH AAA ACN CA-3' as the forward primer and Simt12-Rb: 5'-TGC RGA TAC TTG CAT GTG TAA-3' as the reverse primer. The former was designed with reference to the cytochrome *b* (cyt *b*) gene sequences of *E. fasciatus* (DDBJ/EMBL/GenBank accession number AY786423), *Epinephelus merra* (AY786424), *Epinephelus awoara* (AB108494), *Epinephelus tauvina* (EF456003), *Epinephelus septemfasciatus* (AY786425), *Cephalopholis urodeta* (AY786426) and *Variola louti* (AY786428). The latter was the same as Simt12-Fb, described in Kuriiwa et al. (2007). The amplified region using this primer pair was from the 5' end of the cyt *b* gene to upstream of the 5' of the 12S rRNA gene, thereby including complete sequences of the cyt *b* gene, tRNA-Threonine (tRNA-Thr), tRNA-Proline (tRNA-Pro) and control region (CR).

PCR was carried out with a 10 µl reaction volume containing 1.0 µl of *Ex Taq* Buffer, 0.8 µl dNTP mixture, 0.1 µl of *Ex Taq*® DNA polymerase (TaKaRa), 7.2 µl sterile distilled water, 0.2 µl of each primer (10 µM) and 0.5 µl of template DNA. Amplification parameters were 35 cycles of denaturation at 94 °C for 30 s, annealing at 52 °C for 30 s and extension at 72 °C for 60 s. Double-stranded PCR products, purified using the ExoSAP-IT (USB), were subsequently used for direct cycle sequencing with the BigDye® Terminator Cycle Sequencing Kit ver. 3.1 (Applied Biosystems), following the manufacturer's protocol. Six primers were used for sequencing the PCR products: those described above for PCR and four newly designed (Epi-cyF2: 5'-TAT TCC TAA TAC CAG CAG C-3' and Epi-CRF: 5'-AAG ACA AGG ACT YCT TGA AGG TC-3' as forward primers, and Epi-proR: 5'-GTT TAA TTT AGA ATT CTA GCT TTG G-3' and Epi-cyR: 5'-TTG TCG GCA TCA GAR TTA AGG CC-3' as reverse

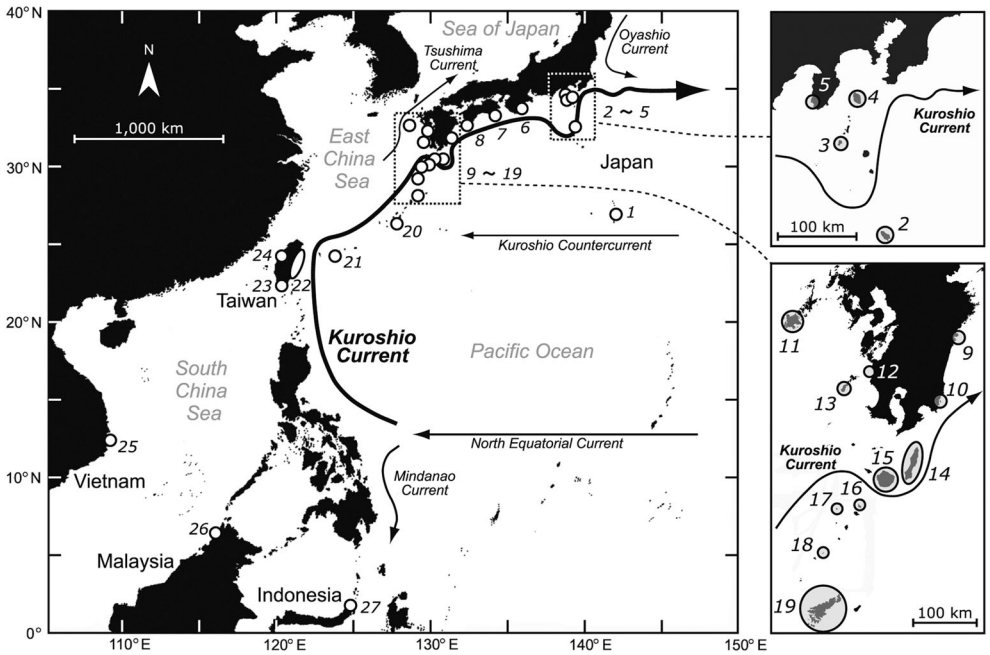

Fig. 2 Collection localities of *Epinephelus fasciatus*. For details of geographic population numbers and number of individuals examined, see Table 1

primers). Dye-labeled fragments were analyzed on a model 3130xl Genetic Analyzer (Applied Biosystems). The DNA sequences were edited and aligned with ATGC ver. 5.0.1 (GENETYX) and MEGA ver. 5.1 (Tamura et al. 2011). All sequences are available from DDBJ/EMBL/GenBank accession numbers AB705627–AB706181 and AB829908–AB829938 (ESM Table S1).

Phylogenetic and haplotype network analyses. A maximum likelihood (ML) tree was inferred by LIKELIHOOD RATCHET (Vos 2003), using all haplotypes of the whole segment sequences of the cyt *b*, tRNA-Thr, tRNA-Pro and CR for *E. fasciatus*. Owing to the long length of the CR sequences for 10 of the 13 outgroups, we succeeded in determining the sequences of only the other three outgroups being adequate for all analyses below. Haplotypes were detected by the program TCS (see outline in haplotype network analysis). Initially, 1,000 trees were generated by the program TNT ver. 1.1 (Goloboff et al. 2008) with 25 % random site-upweighted data, created by the parallel execution program PHYLOGEARS ver. 1.5 (Tanabe 2008). Subsequently, these trees were subjected to a heuristic search using TREEFINDER ver. Oct. 2008 (Jobb et al. 2004; Jobb 2008), with application of the TN93 (Tamura and Nei 1993) + I + Γ model, which was selected as the best-fit model of nucleotide substitution using KAKUSAN ver. 4.0 (Tanabe 2007), on the basis of the partition- and codon-proportional model with Akaike Information Criterion (AIC, Akaike 1973). To account for the difference rate among genes and the codon positions, we divided the whole segment sequences into the following six partitions; the 1st, 2nd, and 3rd codon sites of the cyt *b*, tRNA-Thr, tRNA-Pro and CR. Support for the internal branches of the eventuating tree was assessed using bootstrap resampling with 1,000 replicates by TREEFINDER with PHYLOGEARS.

Phylogenetic trees were also reconstructed by Bayesian phylogenetic analysis, conducted with MRBAYES ver. 3.2.1 (Ronquist et al. 2012), using the same dataset, partitions and AIC parameters. This program can use different nucleotide substitution model on each partition, thus we set the HKY85 (Hasegawa et al. 1985) + I, GTR (Tavaré 1986) + Γ, K80 (Kimura 1980) + I, K80_homogeneous, HKY85 + Γ and GTR + Γ model, which was selected as the best-fit model of nucleotide substitution using KAKUSAN, on the first, second, and third codon sites of the cyt *b*, tRNA-Thr, tRNA-Pro and CR, respectively. Two independent runs of 12,000,000 generations were conducted in each analysis, with tree sampling every 100 generations and burn-in after 12,001 trees. The remaining 108,000 trees from the two independent analyses were used to generate a 50 % majority rule consensus tree, with the percentage of samples recovering any particular clade representing the posterior probability.

On the basis of the average nucleotide substitution rate of the cyt *b* gene and CR, 2 % and 10 % per million years, respectively, between lineages of bony fishes (Bowen et al. 2006b), the divergence time among genetic clades was

Table 2 Genetic variations, results of the neutrality test and demographic indices for sequences of mtDNA cytochrome *b* gene (1,053 bp), control region (872 bp) and whole segment (2,068 bp) within each intraspecific lineage of *Epinephelus fasciatus*

Lineage	*n*	Cyt *b*	CR	Whole segment					
		H	H	H	Φ_{ST}	*h*	$\pi \times 100$	SSD (*P*)	Ragged (*P*)
A	129	19	44	57	0.873	0.931±0.015	0.324±0.170	0.014 (0.408)	0.015 (0.574)
B	386	139	224	291	0.873	0.995±0.001	0.440±0.224	0.002 (0.710)	0.003 (0.890)
C	26	13	21	23	0.872	0.991±0.013	0.358±0.193	0.004 (0.547)	0.013 (0.648)
Total	541	171	289	371	0.872	0.994±0.001	1.594±0.770	-	-

(Continued)

Lineage	Whole segment (continued)					
	Tajima's *D*	Fu's F_S	τ	θ_0	θ_1	θ_1/θ_0
A	-1.444** (0.040)	-24.914* (0.000)	11.012	0.002	12.402	6201.000
B	-2.415* (0.000)	-24.038* (0.002)	10.619	0.009	36.802	4089.111
C	-2.076* (0.000)	-14.144* (0.000)	5.439	1.002	78.750	78.593
Total	-	-	-	-	-	-

Cyt b cytochrome *b*; *CR* control region; *Whole* whole segment of the cyt *b*, tRNA-Threonine, tRNA-Proline and CR; *n* number of individuals examined; *H* number of haplotypes; *h* haplotype diversity; π nucleotide diversity; *SSD* sum of squared deviations; *Ragged* raggedness index; τ units of mutational time; θ_0 population size before expansion; θ_1 population size after expansion

Asterisks (*) and (**) indicate significance at > 99 % and >95 % confidence interval, respectively

Table 3 The average *p*-distance (%) of the cytochrome *b* gene (1,053 bp), control region (872 bp) and whole segment (2,068 bp) sequences within species and each lineage, and between lineages of *Epinephelus fasciatus*

	Within species (range)	Within lineage (range)			Between lineages (range)		
		A	B	C	A and B	A and C	B and C
Cyt *b*	1.2 (0–4.7)	0.2 (0–0.7)	0.4 (0–1.1)	0.2 (0–0.8)	1.9 (1.5–2.5)	3.8 (3.5–4.2)	3.8 (3.4–4.7)
CR	2.0 (0–8.0)	0.6 (0–1.7)	0.6 (0–1.9)	0.6 (0–2.7)	3.1 (2.3–4.5)	7.3 (6.6–8.0)	6.8 (5.9–8.0)
Whole	1.6 (0–5.9)	0.3 (0–0.8)	0.4 (0–1.2)	0.3 (0–1.3)	2.6 (2.2–3.2)	5.6 (5.2–5.9)	4.9 (4.4–5.5)

Cyt b cytochrome *b*; *CR* control region; *Whole* whole segment of the cyt *b*, tRNA-Threonine, tRNA-Proline and CR

roughly estimated. Subsequently, the molecular clock hypothesis was tested with the maximum likelihood method (likelihood ratio test; LRT) using the whole segment sequences for *E. fasciatus* by the BASEML program of PAML ver. 4.7 (Yang 2007). To avoid the computational burden, 50 haplotypes were randomly selected from 371 haplotypes. These consist of Lineages A, B and C. The LRT was carried out on the basis of these data sets and repeated three times independently.

To clarify the historical process of mtDNA haplotypes, a statistical parsimony network in each clade of the phylogenetic tree was constructed by TCS ver. 1.21 (Clement et al. 2000), which employs the method of Templeton et al. (1992). The networks of both the CR and whole segment sequences were too reticulate to detect any structures (data not shown), so that we used the cyt *b* gene sequences for all individuals of *E. fasciatus*. The networks were connected using a maximum parsimony algorithm, with a statistical confidence of 95 %. The ancestral haplotype was also identified using TCS by the method of Castelloe and Templeton (1994), which estimates outgroup-weights based on haplotype frequency and connectivity, the haplotype with the highest outgroup-weight most likely being the oldest.

Demographic analyses and population structure. The program ARLEQUIN ver. 3.11 (Excoffier et al. 2005) was used to generate haplotype diversity (*h*) and nucleotide diversity (π) of the whole segment sequences within genetic clades. This program was also used for the following analyses and tests. Theoretical distributions under simulated constant population size and a sudden expansion model (Rogers and Harpending 1992) were compared to the goodness-of-fit of the observed data with the sum of squared deviations (SSD) and raggedness indices (Herpending 1994). Neutrality of the sequence variation of each genetic clade was verified using Tajima's *D* (Tajima 1989) and Fu's F_S (Fu 1997) tests. To estimate demographic parameters, pairwise mismatch distributions (Rogers and

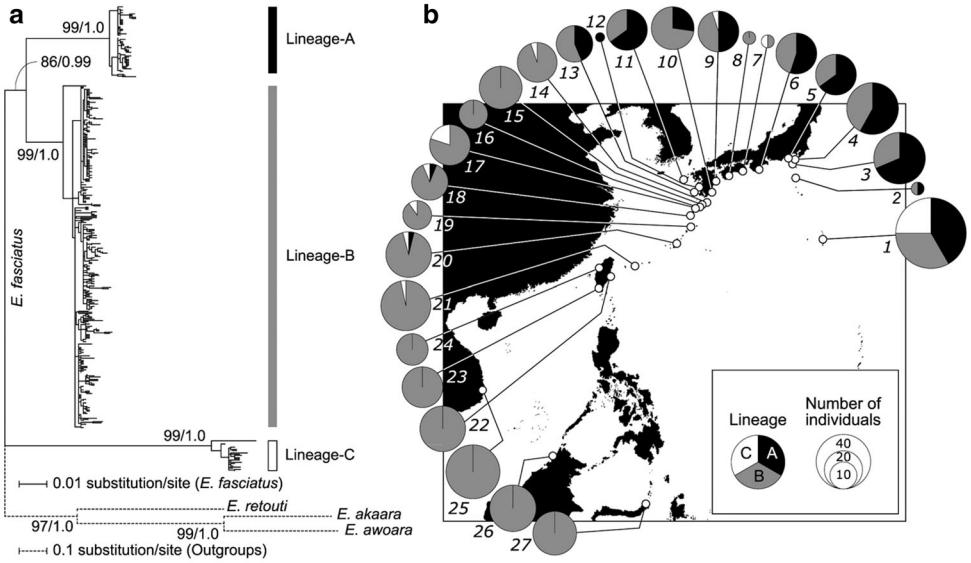

Fig. 3 Phylogenetic tree and geographic distribution of intraspecific lineages for *Epinephelus fasciatus*. **a** Maximum likelihood (ML) tree based on whole segment sequences of mtDNA cytochrome *b* gene, tRNA-Threonine, tRNA-Proline and control region from 371 haplotypes using the TN93+ I + Γ model of sequence evolution on the basis of the partition- and codon-proportional model with Akaike Information Criterion. Numerals above nodes indicate bootstrap values in the ML (left) and posterior probabilities in the Bayesian trees (right) from 1,000 replicates. *Solid and dotted line scale* indicates 0.01 % (*E. fasciatus*) and 0.1 % (outgroups) substitution per site, respectively; **b** geographic distribution of intraspecific lineages of *E. fasciatus*. *Each color code of circle* refers to three lineages in the phylogenetic tree (**a**). *Circle size* proportional to number of individuals. For details of geographic population numbers beside open circles and number of individuals examined, see Table 1 and ESM Table S2

Harpending 1992) were calculated within genetic clades. The times and magnitudes of inferred sudden expansions were determined by calculating τ (assuming $\tau = 2\ ut$, where u is the mutation rate per generation for the entire region of DNA under study and t is the time in generations), θ_0 and θ_1 (assuming $\theta_0 = 2\ N_{0\mu}$ and $\theta_1 = 2\ N_{1\mu}$, where N_0 and N_1 are the population sizes before and after expansion, and μ is the mutation rate per nucleotide), using a set of 1,000 parametric bootstrap replicates (Rogers and Harpending 1992; Rogers 1995; Schneider and Excoffier 1999; Excoffier 2004).

The Bayesian skyline plot (BSP; Drummond et al. 2005) for each genetic clade was carried out to clarify past dynamics in the female effective population size (N_{ef}) through time, using BEAST ver. 1.7.5 (Drummond and Rambaut 2007). The best-fit model of nucleotide substitution for whole segment sequences was selected using KAKUSAN. Each Markov chain Monte Carlo (MCMC) process was based on a run of 10,000,000 generations, and genealogies were sampled every 1,000 generations. Ten percent of sampled genealogies were discarded as burn-in. On the basis of the harmonic mean of nucleotide divergence rates of the cyt *b* gene and CR between lineages of bony fishes (Bowen et al. 2006b), nucleotide substitution rate of 3.3 % per million years was applied under the strict molecular clock model based on the results of the LRT analyzed by BASEML. Convergence for the posterior means of all parameters was assessed using TRACER ver. 1.5 (Rambaut and Drummond 2009) by checking $N_{ef} > 200$.

The genetic structure for each of 23 geographic populations, which included more than 10 individuals, was assessed by an analysis of molecular variance AMOVA (Excoffier et al. 1992), as implemented in ARLEQUIN. The diversity measure Φ-statistics values were calculated using the whole segment sequences. The criterion for significant differences of pairwise Φ_{ST} (genetic differences between populations) values from zero among the 23 geographic populations was tested by a nonparametric permutation test (Rice 1989). Population grouping based upon genetic variability was performed by SAMOVA ver. 1.0 (Dupanloup et al. 2002), which pooled populations into alternative structures by maximizing Φ_{CT} (genetic differences among the population groups) values.

Results

Genetic variation. DNA segments of 2,061–2,068 bp were successfully sequenced for all 541 individuals of *Epinephelus fasciatus*. These included partial sequences of the cyt *b* gene (1,053 bp) and complete sequences of the tRNA-Thr (73 bp), tRNA-Pro (69–70 bp) and CR

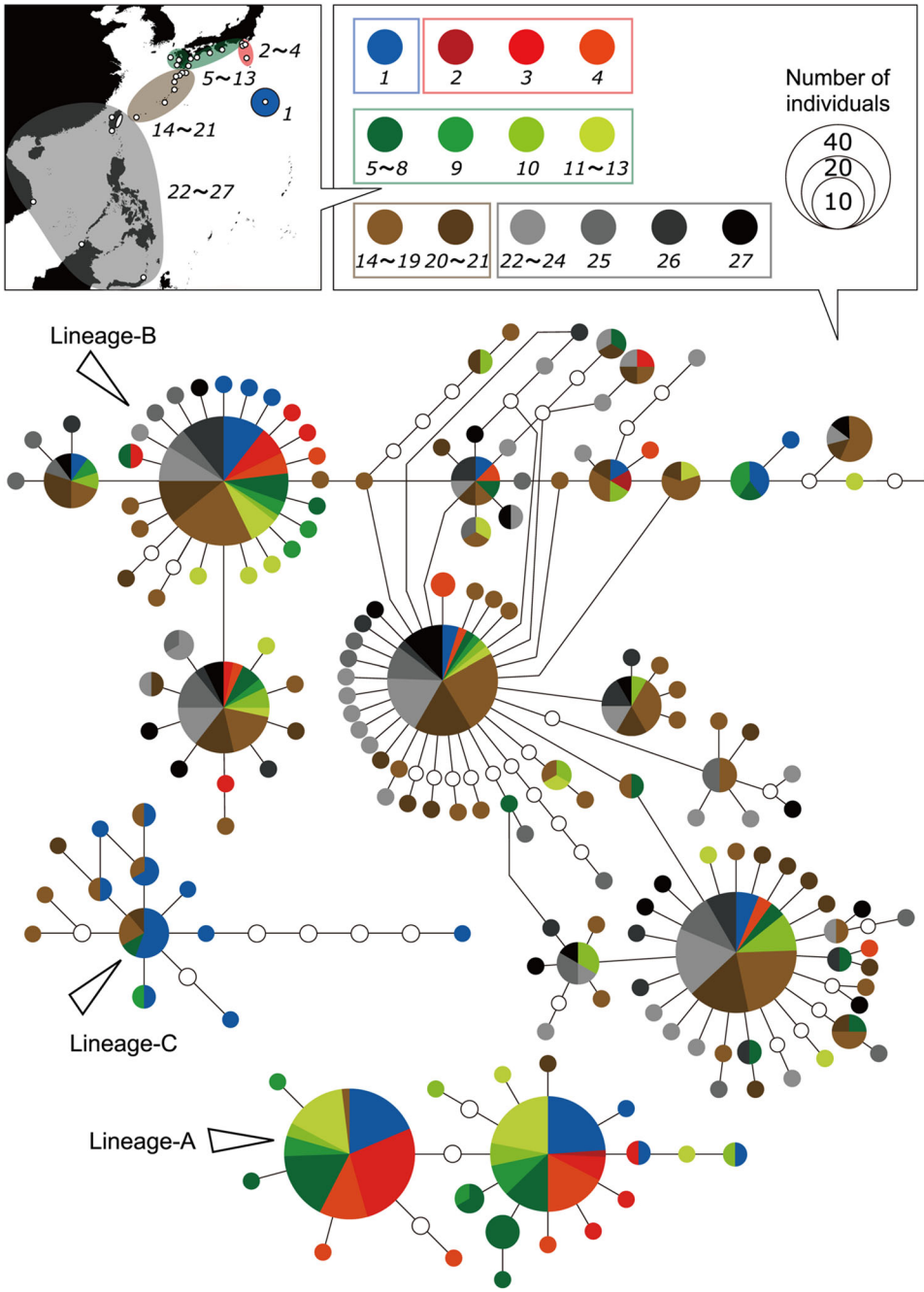

Fig. 4 Haplotype networks of the cytochrome *b* gene sequences from all 541 individuals of intraspecific lineages for *Epinephelus fasciatus*. *Circles* connected to one another represent mtDNA haplotypes of cytochrome *b* gene sequences (1,053 bp). *Circle size* is proportional to haplotype frequency. *Small open circles* represent putative (missing) haplotypes not detected in this study. *Color codes of each circle* refer to geographic populations in map (above). *Solid arrow* indicates highest outgroup-weight haplotype in each lineage

(866–872 bp). A total of 170 (cyt *b*), 8 (tRNA-Thr), 6 (tRNA-Pro), 229 (CR) and 413 (whole segment) nucleotide positions varied within the species, such variations defining 171 (cyt *b*), 9 (tRNA-Thr), 6 (tRNA-Pro), 289 (CR) and 371 (whole segment) haplotypes (Table 2). The same regions of DNA segments for three outgroups (*E. retouti*, *E. akaara* and *E. awoara*) were also determined (2,184–2,293 bp), only the cyt *b* gene sequences being determined for the remaining ten due to the long length of their CR sequences (ESM Table S1). The average *p*-distance (uncorrected sequence divergence) of the cyt *b*, CR and whole segment sequences within *E. fasciatus* are shown in Table 3. That of the cyt *b* was 14.9 % (range 9.6–16.3 %) between *E. fasciatus* and 13 outgroups, and

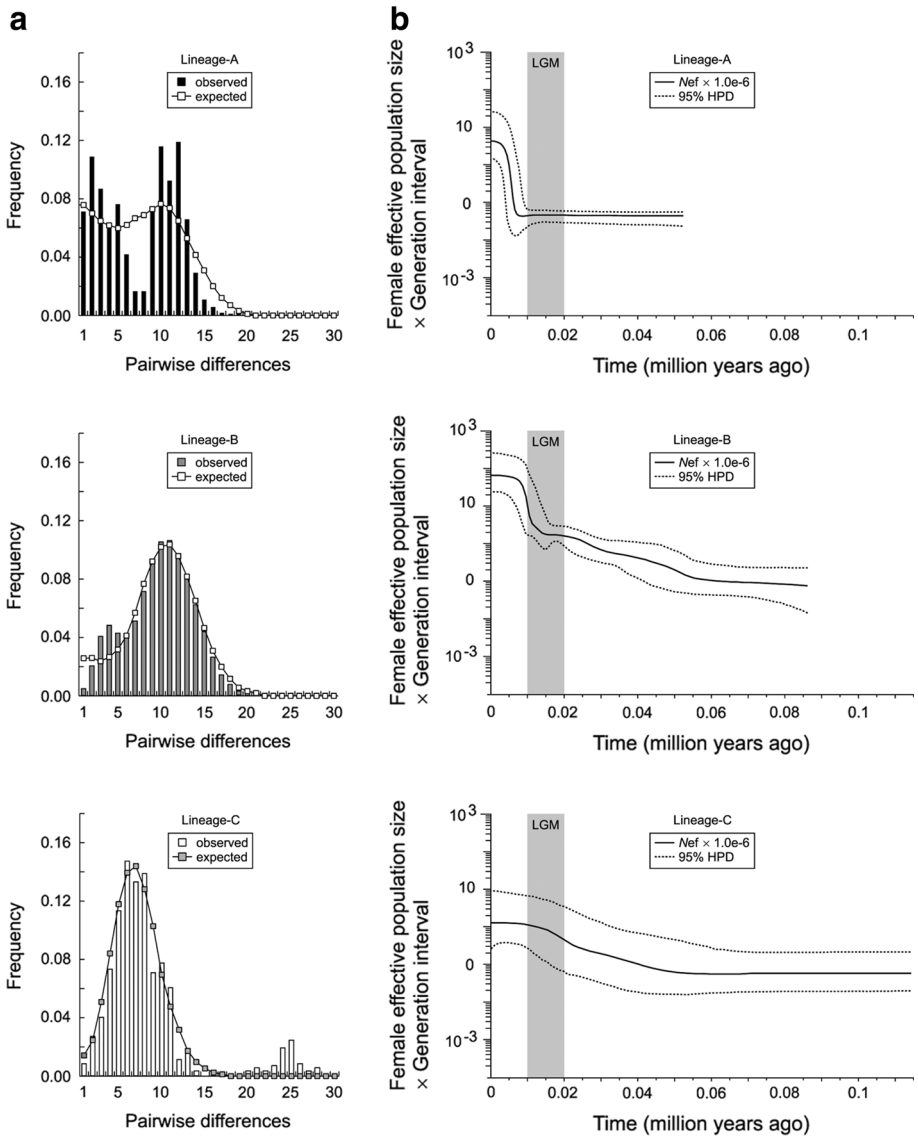

Fig. 5 Mismatch distributions and Bayesian skyline plots (BSPs) from all 541 individuals of intraspecific lineages for *Epinephelus fasciatus*. **a** Observed (*vertical bars*) and expected (*solid lines*) mismatch distribution of pairwise sequence divergence for whole segment sequences of mtDNA cytochrome *b* gene, tRNA-Threonine, tRNA-Proline and control region. *Horizontal and vertical axes* indicate genetic differences and frequency, respectively. *Each color code* refers to each lineage in the phylogenetic tree (Fig. 3a); **b** BSPs from the same dataset of mismatch distributions. *Horizontal axis* represents time in million years ago and *vertical axis* representing the female effective population size (N_{ef}) × generation interval (10^{-6} million years ago) is given on a logarithmic scale. *Solid and dotted lines* represent mean $N_{ef} \times 10^{-6}$ and 95 % highest probability density (HPD) intervals, respectively. *Inserted gray regions* indicate the Last Glacial Maximum (LGM; ca. 0.01–0.02 million years ago)

14.1 % (6.0–16.5 %) among the 13 outgroups. That of the CR and whole segment sequences between *E. fasciatus* and three outgroups was 20.3 % (17.2–23.6 %) and 16.5 % (14.4–18.4 %), and among three outgroups was 23.9 % (20.9–25.5 %) and 17.0 % (13.5–19.0 %), respectively.

Phylogenetic relationships. The phylogenetic analyses using the 371 haplotypes of the whole segment sequences revealed that *E. fasciatus* was divided into three highly supported genetic clades (Fig. 3a; ESM Fig. S1), referred to here as intraspecific lineages A, B and C. Both the ML and Bayesian analyses produced an identical topology. Each lineage consisted of 57 haplotypes for 129 individuals (Lineage A), 291 for 386 (B) and 23 for 26 (C), from many geographic populations (Fig. 3b; Table 2; ESM Table S2). The average *p*-distance of the cyt *b*, CR and whole segment sequences within a single lineage and between lineages are listed in Table 3. The divergence time of lineages A/B and AB/C of *E. fasciatus* was roughly estimated as having been 0.95 and 1.90 (cyt *b*), and 0.31 and 0.71 (CR) million years ago (MYA), respectively. The strict molecular clock hypothesis could not be rejected in every trial of the LRT analyses ($P > 0.05$; ESM Table S3).

Haplotype network. Haplotype networks of the cyt *b* gene sequences for the three lineages are shown in Fig. 4. Those for Lineage A exhibited two dominant haplotypes with several rare haplotypes that differed by less than three mutational steps. The two dominant haplotypes were connected by two mutational steps. The network for Lineage B was more complex, consisting of four dominant haplotypes, connected by one to two mutational steps, and numerous rare haplotypes that differed by less than six mutational steps. Although the number of individuals was insufficient for determining a definite structure, the Lineage C network included a single dominant haplotype with several rare (one highly differentiated) haplotypes.

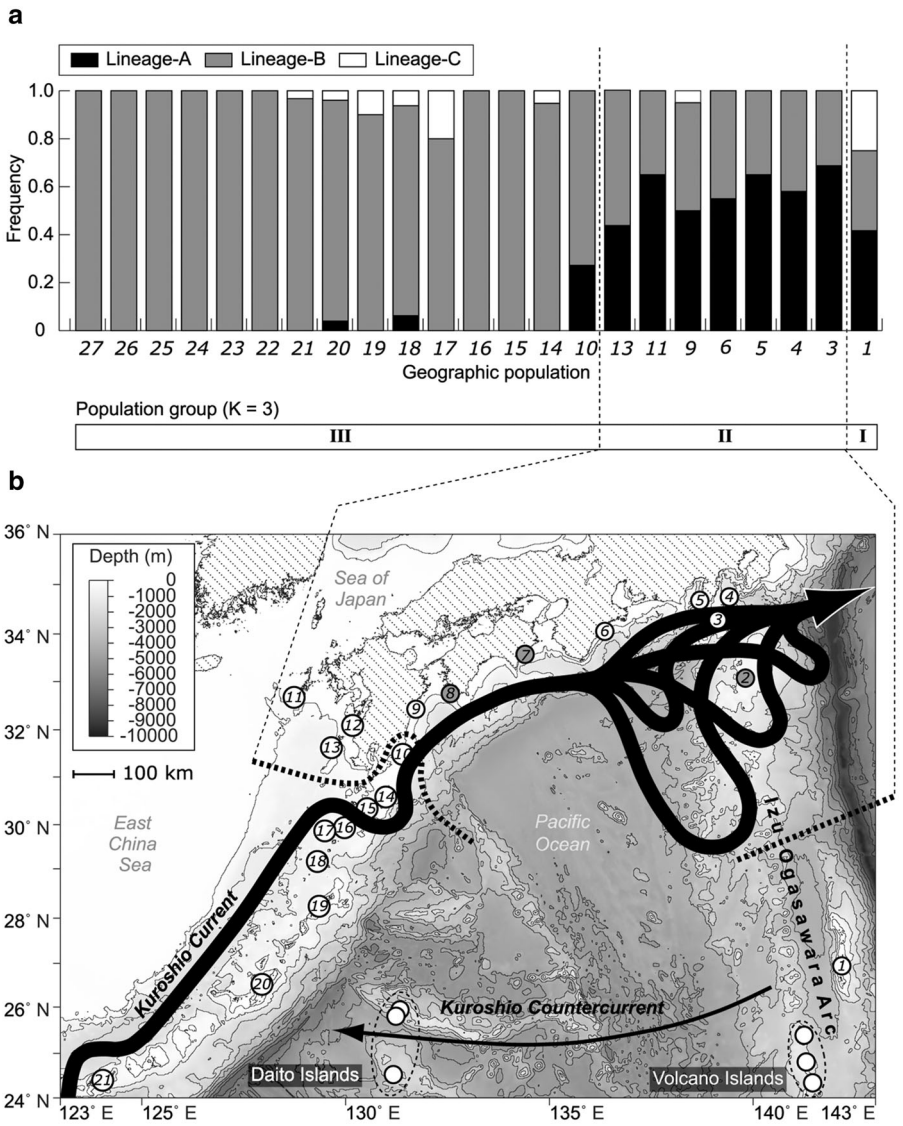

Fig. 6 Phylogeographic provinces of *Epinephelus fasciatus*. **a** Frequency of intraspecific lineages in 23 geographic populations (above) and phylogeographic provinces indicated by population grouping (below). *Geographic population numbers* (oblique) and *color codes* refer to Table 1 and Fig. 3, respectively. K value indicates number of groups for maximizing genetic differences among population groups, Φ_{CT} values. *Roman numerals* indicate population group numbers. For details of population grouping, see ESM Table S3; **b** *bold and thin arrows* represent routes of the Kuroshio Current and Kuroshio Countercurrent, respectively. *Dotted lines* indicate phylogeographic boundaries with reference to phylogeographic provinces of *E. fasciatus* (**a**). *Geographic population numbers* inside open circles refer to Table 1

Demographic analyses. The demographic analyses using the whole segment sequences showed a historical demography of each lineage. Although the haplotype diversity (h) was very high ($h = 0.931$–0.995), nucleotide diversity (π) was low ($\pi = 0.003$–0.004) in all lineages (Table 2), suggesting sudden expansions after bottleneck effects. Neutrality tests also showed evidence of sudden expansions in all lineages; insignificant SSD values and raggedness indices ($P > 0.05$), and significant Tajima's D and Fu's F_S values ($P < 0.05$) occurred for all lineages (Table 2).

Although mismatch distributions in Lineage B were unimodal and consistent with an expanding population size, Lineages A and C represented bimodal distributions (Fig. 5a). In the bimodal distribution of Lineage A, two peaks were connected with a continual degree of pairwise differences. In that of Lineage C, the lower peak was caused by a highly differentiated individual, reflecting the phylogenetic tree and haplotype network (Figs. 3a, 4, 5a).

The BSPs showed that the population expansion dynamics in each lineage at approximately 0.05 (Lineage A), 0.085 (B) and 0.115 (C) MYA of the coalescent time for the most recent common ancestor (MRCA), respectively, from the analysis with the strict molecular clock model (Fig. 5b). The BSPs also showed that the N_{ef} clearly departed from the constant population size model in each lineage (Fig. 5b). In Lineage A, although the BSP did not show departure from the constant size model before the Last Glacial Maximum (LGM; ca. 0.01–0.02 MYA), the N_{ef} expanded notably after the LGM. The BSP in Lineage B showed gradual increase before the LGM but notable

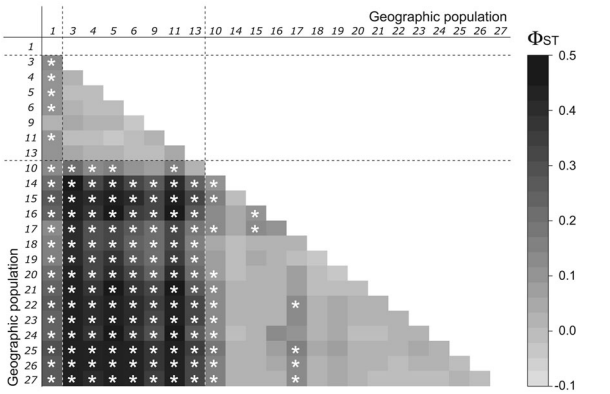

Fig. 7 Color-coded visible columns of pairwise Φ_{ST} values among 23 geographic populations of *Epinephelus fasciatus*. *Each color code* refers to degree of Φ_{ST} values (right). *Asterisks* indicate significance at 95 % confidence interval. *Geographic population numbers* (oblique) refer to Table 1. *Dotted lines* indicate phylogeographic boundaries of *E. fasciatus* (Fig. 6a). Raw data of pairwise Φ_{ST} and *P* values refer to ESM Table S5. The style of this figure was referred to that of fig. 2 given by Hickey et al. (2009)

after the LGM. On the contrary, that in Lineage C was consistently and gradually increasing, being not related to the LGM.

Demographic indices using the whole segment sequences indicated the time and magnitude of expansion of each lineage (Table 2). The observed τ value of Lineage C was smaller than in Lineages A and B, indicating that the time at which expansion started was later in Lineage C than in the other two lineages. Although the estimated effective population size before expansion (θ_0) in Lineage C was much greater than zero, whereas those in Lineages A and B equaled approximately zero, the paces of expansion (θ_1/θ_0) in Lineages A and B were greater than in Lineage C. A comparison of the θ_1 values suggested that the present population size of Lineage C is the largest, that of Lineage A being the smallest.

Population structure. Each geographic population consisted of individuals of the three genetic lineages, albeit in different ratios (Figs. 3b, 6a; ESM Table S2). Twenty-three geographic populations were divided into three demographic groups (Groups I, II and III) by SAMOVA analyses (Fig. 6a; ESM Table S3), in which the K value (number of groups) = 3 was selected by maximizing Φ_{CT} values ($\Phi_{CT} = 0.342$, $\Phi_{SC} = 0.003$, $\Phi_{ST} = 0.344$). Group I consisted of a population from the Ogasawara Islands (population-1), including individuals of all three lineages, each in an approximately equal ratio. Group II included both of the geographic populations from the Izu Islands (3 and 4) and most from the main islands of Japan (5, 6, 9, 11 and 13), including primarily individuals of Lineage A, but also those of Lineage B. Group III consisted of a population from the main islands of Japan (10) (dominated by individuals of Lineage B but also including those of Lineage A), and populations from the Ryukyu Islands (14–21) and all countries sampled south of Japan (22–27), all of which comprised individuals of Lineage B only. Mismatch distributions of 23 geographic populations and three demographic groups are shown in ESM Figs. S2 and S3, respectively. In those, the number of peaks for pairwise differences depended on the number of genetic lineages being included in each geographic population and demographic groups.

The three demographic groups were also supported by the results of the population pairwise Φ_{ST} analyses (Fig. 7; ESM Table S4). Most of the significant differentiation found occurred among groups ($\Phi_{ST} = 0.071$–0.558; $P < 0.05$), rather than within groups, the exception being population-10. Although this population was included in Group III, a significant differentiation was found not only between populations of Group I ($\Phi_{ST} = 0.117$; $P < 0.01$) and II ($\Phi_{ST} = 0.107$–0.218; $P < 0.05$), but also between other populations of Group III ($\Phi_{ST} = 0.067$–0.159; $P < 0.05$).

Discussion

Evolutionary history of *E. fasciatus*. The molecular phylogenetic and demographic analyses indicated that *Epinephelus fasciatus* distributed in Japanese waters and the tropical western Pacific is genetically clustered into three cryptic intraspecific lineages (Fig. 3a: Lineages A, B and C), which exhibit different evolutionary histories.

Lineage A (termed the "Japanese lineage") probably became differentiated in Japanese waters in the early middle Pleistocene (ca. 0.13–2.59 MYA) under the influence of long-period fluctuations in the route of the Kuroshio Current (Fig. 3a). During the Pleistocene (ca. 0.01–2.59 MYA), land bridges connecting the main islands of Japan to continental Asia, and the central-southern Ryukyu Islands to continental Asia via Taiwan, appeared and disappeared several times (Ota 1998; Kimura 2000). When land bridges appeared, especially during the LGM (ca. 0.01–0.02 MYA), the ancient Kuroshio Current turned to the east at the southern end of the Ryukyu Islands (Ujiié and Ujiié 1999; Ujiié et al. 2003). When land bridges disappeared, however, the ancient Kuroshio Current may have flowed northward via the southern tip of the Ryukyu Islands and Taiwan, a route similar to that of the present day. The continual bimodal distribution in a mismatch analysis and the population expansion after the LGM in the BSP of Lineage A (Fig. 5a, b) suggested that some populations dispersed and were isolated when land bridges appeared, and subsequently experienced the secondary contact when they disappeared after the LGM.

Although individuals of Lineage B, here termed the "northwestern Pacific lineage", were found in all

geographic populations and those of Lineages A and B were sympatric in Japanese waters (Figs. 3b, 6a), the northern individuals of Lineage B were primarily found in the Ryukyu Islands, their distribution extending northward to the coast of the main islands of Japan through transportation by the Kuroshio Current. An alternative scenario, based on differences in adaptive abilities, such as tolerance to cold temperatures, might also be considered. Individuals of Lineages A and B were in greater proportion in the temperate region (main islands of Japan) with the opposite being true for the tropical/subtropical region (Ryukyu Islands). A comparison of the ratios of these two lineages between populations 9 vs 10, 11 vs 13, 9 vs 11 and 10 vs 13, showed that of Lineage B to be higher than that of Lineage A in the area strongly influenced by the Kuroshio Current and thereby characterized by a higher temperature (Fig. 6). However, in the subtropical Ogasawara Islands (population-1), individuals of these two lineages were found in almost equal ratio. Given these data, the northward dispersal of Lineage B by the Kuroshio Current is a reasonable hypothesis. The BSP of Lineage B suggested that the ancient Kuroshio Current was mainly influenced only in the Ryukyu Islands and the northernmost individuals of Lineage B were distributed in the Ryukyu Islands until the LGM. However, the route of the Kuroshio Current changed to the present flow after the LGM, expanding the distribution and the population size of *E. fasciatus* (Fig. 5b). The distributions of Lineages A and B extended along the route of the Kuroshio Current (Fig. 3b), and all dominant haplotypes in the haplotype networks for these two lineages occur in individuals from most geographic populations (Fig. 4). This implies that most of the dominant haplotypes existed before expansion of the populations with large geographic-scale gene flow occurring after expansion due to current-assisted transport of individuals.

The evolutionary history of Lineage C most likely differs from those of the other two lineages due to the geographic distribution of the former. The Ogasawara Islands, where most of the individuals of Lineage C were found, are typical oceanic islands and not strongly influenced by the Kuroshio Current. The BSP of Lineage C suggested that not only the present day current but also the ancient one did not influence the islands (Fig. 5b). In addition, the center of distribution of Lineage C appears to be outside the area from which the present specimens were sampled, although many individuals of this lineage were found in the Ogasawara Islands (Fig. 3b; ESM Table S2). This reasoning was based on the large value for the estimated population size of Lineage C after expansion, in spite of the lineage being represented by the lowest number of individuals sampled (Table 2). The most differentiated individual (Figs. 3a, 4, 5a) may also support the hypothesis. We suspect that individuals of Lineage C are mainly distributed in the Mariana Islands, located on the eastern edge of the Philippine Sea Plate. Not only did Springer (1982) propose a pattern of distribution and endemicity of shorefish species associated with that tectonic plate, but also Randall et al. (1997) demonstrated an affinity of fish faunas between the Ogasawara and Mariana islands. Specimens from the Mariana Islands are required for clarification of the distribution pattern of Lineage C.

Interestingly, the three genetic lineages are not distinguishable by body coloration or maximum body size. Individuals a–c, d–f and g–i in Fig. 1, belonging, respectively, to Lineages A, B and C, clearly illustrated that each genetic lineage includes all color variations. We note that orange or whitish individuals were found in tropical/subtropical regions and reddish ones in temperate regions suggesting that coloration may be related to habitat factors rather than mitochondrial DNA lineages. Aquacultured individuals of *E. fasciatus* in the Ogasawara Islands provided a clue with hatchery-reared juveniles being dark brown (ESM Fig. S2), changing to red-, orange- or white-tinged within a year of their release (unpublished observation by the Tokyo Metropolitan Ogasawara Fisheries Research Center). This suggests that coloration of *E. fasciatus* may be influenced by diet.

Maximum body size (ESM Table S6) may also be related to habitat factors, most likely water temperature and the length and/or times of reproduction. Recent studies of hatchery-reared *E. fasciatus* revealed that the length of the spawning period in a subtropical region (Ogasawara Islands) was more than twice that in temperate waters (main islands of Japan) (Kawabe et al. 2000). In addition, the spawning frequency of individuals in the Ogasawara Islands is possibly more than once per season (unpublished observation by the Tokyo Metropolitan Ogasawara Fisheries Research Center). Moreover, the average diameter of pelagic eggs and the total length of larval *E. fasciatus* have a significant negative correlation with increasing water temperature (Kawabe et al. 2000; Kawabe 2005). Individuals living in temperate regions may, therefore, grow larger than those in tropical/subtropical regions.

The sympatric occurrences of the three DNA lineages at the collection sites suggested that individuals can successfully interbreed irrespective of their genetic lineages. An analysis of 32 hatchery-reared *E. fasciatus* individuals from the Fisheries Cooperative Association of Chichi-jima Island (Ogasawara Islands), which were randomly selected from clutches spawned in 2004–2007, found all three lineages, in the ratio A:B:C = 13:18:1. In that fisheries cooperative, spawned eggs are obtained from several hundred, multi-generational adult fish, implying an absence of genetic incompatibility among the DNA lineages.

Genetic population structure of *E. fasciatus*. The present study of *E. fasciatus* from many localities in

Japanese waters and the tropical western Pacific revealed the distinctive genetic population structure of the species, its uniqueness lying in the occurrence of individuals of three mitochondrial DNA lineages having sympatric distributions with different lineage ratios in each geographic population, hence three demographic groups (I, II and III) (Figs. 3b, 6a). Such a complex structure in a species of pelagic larval duration (PLD) approximately two months comes as a surprise because the larvae may be able to disperse over a long distance. Many previous studies have investigated the relationships between PLD and genetic population structure in marine fishes, those having a short or no PLD generally exhibiting an obvious genetic structure (e.g., Riginos and Nachman 2001), whereas those with a lengthy PLD may have a non-significant genetic structure. The population structure in marine fishes may be determined not only by PLD but also larval retention and self-recruitment (Jones et al. 1999; Swearer et al. 1999; Almany et al. 2007), adult habitat preference (Rocha et al. 2002), historical vicariance (Bernardi et al. 2003; Shirai et al. 2006; Liu et al. 2007), dispersal ability and endemic distribution (Bowen et al. 2006a; Eble et al. 2009), ocean currents (Rocha et al. 2008) and genetic isolation-by-distance (Hickey et al. 2009). In the case of *E. fasciatus* in Japanese waters, the dual roles of the Kuroshio Current, those of a transport system and an unseen marine barrier, may contribute concurrently in determining the population structure. The phylogeographic pattern suggested that individuals of Lineage B can disperse from the Ryukyu Islands and tropical western Pacific (Group III) to the main islands of Japan (II), transported by the Kuroshio Current. However, those of Lineage A cannot be transported from north to south, due to the Kuroshio Current barrier (Fig. 6a, b).

It has been well established that the Kuroshio Current fluctuates greatly both north and south of the central island (Honshu) of Japan being classified into five types (Fig. 6b; data from the Hydrographic and Oceanographic Department, Japan Coast Guard). Such fluctuations provide for both dispersal and migration of marine fishes along the coast of the central island of Japan and the Izu Islands, and sometimes also the Ogasawara Islands (Senou et al. 2006). Although the distribution of individuals of Lineages A and B in Fig. 6a strongly supports a hypothesis of fish dispersal from north to south (from Group II to I), dispersal in the opposite direction (from I to II) was not indicated by the distribution of Lineage C. Several endemic species in the Ogasawara Islands including *Chaetodon daedalma* and *Scarus obishime* have been often found in the southern part of the Izu Islands (Senou et al. 2002, 2006), supporting an hypothesis of fish dispersal from south to north. However, opportunities for northward and southward dispersal differ: whereas the Kuroshio Current may play a positive role in southward transport along the Izu-Ogasawara (Bonin) Arc (see below), it may act as a weak barrier for northerly dispersal. This hypothesis cannot be further investigated here due to an insufficient number of individuals obtained from Hachijo-jima Island (population-2) (southern Izu Islands).

In addition to the dual roles of the Kuroshio Current mentioned above, a geographic factor is also thought to contribute to the population structure between the Izu and Ogasawara islands, which together constitute the Izu-Ogasawara Arc, expanding for approximately 1,200 km from Honshu Island to the Volcano Islands (Fig. 6b). Generally, dispersed larvae cannot survive unless they find shallow coastal or island waters to settle, which suggests the "stepping stone theory" (see "stepping stone model" of population structure in Kimura and Weiss 1964). It is, therefore, reasonable to consider that fish larvae transported by the Kuroshio Current can survive in this island arc. Moreover, not only larvae but also adult fishes may be able to migrate along this island arc.

Several exceptional individuals representing Lineages A and C in the Ryukyu Islands population (Figs. 3b, 6a) indicated that larval dispersal of *E. fasciatus* rarely occurs from the Ogasawara Islands to the Ryukyu Islands. Despite a weak westerly current (Kuroshio Countercurrent), its unsettled nature and lack of major island "stepping stones", except for the Daito (Borodino) Islands comprising several very small islands in the extensive area covering some 1,400 km between the two island groups (Fig. 6b), make for difficult westward movement for most fishes. However, a few species of coral reef fishes have been reported as having been transported from the Ogasawara Islands to the Daito and/or Ryukyu islands: *Chaetodon daedalma* (see Yoshigou 2004), *Hemitaurichthys thompsoni* (see Shimada 2002) and *Ctenochaetus hawaiiensis* (see Senou et al. 2003). We, therefore, consider that *E. fasciatus*, having a lengthy PLD, may disperse accidentally by means of the Kuroshio Countercurrent.

Marine biogeographic boundaries with reference to fishes in Japanese waters. An additional finding of this study was that the genetic population breaks in *E. fasciatus* (Fig. 6a, b) coincided with the marine biogeographic boundaries (with reference to the fish fauna in Japanese waters), proposed by Matsuura and Senou (2012). Cluster analyses of fish fauna by them revealed that 12 regions in southern Japan were grouped into two clusters: the first comprising islands located in the Ryukyu Islands, and the other comprising the main islands of Japan, and the Izu and Ogasawara islands. In the latter cluster, a weak faunal break was found between the Izu and Ogasawara islands.

Acknowledgements We express our sincere gratitude to the following persons and organizations for helping in the collection of

fishes: Y. Iwatsuki (MUFS); K.T. Shao (Research Center of Biodiversity, Academia Sinica, Taiwan); H.C. Ho (National Museum of Marine Biology and Aquarium, Taiwan); W.C. Jiang and colleagues (Eastern Marine Biology Research Center, Fisheries Research Institute, Taiwan); S. Kimura (FRLM); G. Ogihara and M. Matsunuma (KAUM); G. Shinohara, Y. Takata and M. Nakae (NSMT); Y. Sakurai (Okinawa Environmental Research Co. Ltd.); A. Murase and H. Arihara (Tokyo University of Marine Science and Technology); M. Mizukami (Fukuyama University); N. Akama, Y. Matsue, E. Nagao and Y. Minagawa (professional fishermen on Hachijo-jima, Kozu, Fukue, and Ishigaki-jima Island, respectively); Ogasawara Diving Service KAIZIN; Ogasawara Flippers Inn; and the Fisheries Cooperative Associations on Chichi-jima Island, Minami-Izu-machi, Goto Islands, Tanegashima Island and Yaku-shima Island. We also thank K. Kawabe (Tokyo Metropolitan Ogasawara Fisheries Research Center) for useful information about ecology of *E. fasciatus* and T. Yonezawa (Fudan University, China) for helping phylogenetic and demographic analyses. We are grateful to G.S. Hardy (Ngunguru, New Zealand) and E. Murdy (George Washington University) for their help with English. This study was supported by a Grant-in-Aid for Scientific Researches (A) and (B) from the Japan Society for the Promotion of Science (A: 19208019, B: 24370041), a Grant-in-Aid for Young Scientists (B) from the Ministry of Education, Science, Sports and Culture, Japan (22770089) and the Kuroshio Project of the National Museum of Nature and Science.

References

Akaike H (1973) Information theory and an extension of the maximum likelihood principle. In: Petrov BN, Csaki F (eds) Second international symposium on information theory. Akademiai Kiado, Budapest, Hungary, pp 267–281

Almany GR, Berumen ML, Thorrold SR, Planes S, Jones GP (2007) Local replenishment of coral reef fish populations in a marine reserve. Science 316:742–744

Avise JC (2000) The history and purview of phylogeography. In: Avise JC (ed) Phylogeography: The history and formation of species. Harvard University Press, Cambridge, pp 3–36

Bernardi G, Findley L, Rocha-Olivares A (2003) Vicariance and dispersal across Baja California in disjunct marine fish populations. Evolution 57:1599–1609

Bowen BW, Bass AL, Mus A, Carlin J, Robertson DR (2006a) Phylogeography of two Atlantic squirrelfishes (Family Holocentridae): exploring links between pelagic larval duration and population connectivity. Mar Biol 149:899–913

Bowen BW, Muss A, Rocha LA, Grant WS (2006b) Shallow mtDNA coalescence in Atlantic pygmy angelfishes (Genus *Centropyge*) indicates a recent invasion from the Indian Ocean. J Hered 97:1–12

Briggs JC (1974) Chapter 8: Northern Hemisphere Warm-Temperate Regions, and Chapter 9: Northern Hemisphere Cold-Temperate Regions. In: Briggs JC (ed) Marine Zoogeography. McGraw-Hill, Inc., New York, pp 196–245, 247–297

Castelloe J, Templeton A (1994) Root probabilities for intraspecific gene trees under neutral coalescent theory. Mol Phylogenet Evol 3:102–113

Clement M, Posada D, Crandall KA (2000) TCS: A computer program to estimate gene genealogies. Mol Ecol 9:1657–1659

Craig MT, Hastings PA (2007) A molecular phylogeny of the groupers of the subfamily Epinephelinae (Serranidae) with a revised classification of the Epinephelini. Ichthyol Res 54:1–17

Drummond AJ, Rambaut A (2007) BEAST: Bayesian evolutionary analysis by sampling trees. BMC Evol Biol 7:214

Drummond AJ, Rambaut A, Shapiro B, Pybus OG (2005) Bayesian coalescent inference of past population dynamics from molecular sequences. Mol Biol Evol 22:1185–1192

Dupanloup I, Schneider S, Excoffier L (2002) A simulated annealing approach to define the genetic structure of populations. Mol Ecol 11:2571–2581

Eble JA, Toonen RJ, Bowen BW (2009) Endemism and dispersal: comparative phylogeography of three surgeonfishes across the Hawaiian Archipelago. Mar Biol 156:689–698

Excoffier L (2004) Patterns of DNA sequence diversity and genetic structure after a range expansion: lessons from the infinite-island model. Mol Ecol, 13:853–864

Excoffier L, Laval G, Schneider S (2005) ARLEQUIN ver. 3.0: an integrated software package for population genetics data analysis. Evol Bioinform Online 1:47–50

Excoffier L, Smouse PE, Quatro JM (1992) Analysis of molecular variance inferred from metric distances among DNA haplotypes: application to human mitochondrial DNA restriction data. Genetics 131:479–491

Fu YX (1997) Statistical neutrality of mutations against population growth, hitchhiking and background selection. Genetics 147:915–925

Fujikura K, Lindsay D, Kitazato H, Nishida S, Shirayama Y (2010) Marine biodiversity in Japanese waters. PLoS One 5(8):e11836

Goloboff PA, Farris JS, Nixon KC (2008) TNT, a free program for phylogenetic analysis. Cladistics 24:774–786

Grant WS, Bowen BW (1998) Shallow population histories in deep evolutionary lineages of marine fishes: insights from sardines and anchovies and lessons for conservation. J Hered 89:415–426

Hasegawa M, Kishino H, Yano T (1985) Dating of the human-ape splitting by a molecular clock of mitochondrial DNA. J Mol Evol 22:160–174

Herpending HC (1994) Signature of ancient population growth in a low resolution mitochondrial DNA mismatch distribution. Hum Biol 66:591–600

Hickey AJ, Lavery SD, Hannan DA, Scott-Baker C, Clements KD (2009) New Zealand triplefin fishes (family Tripterygiidae): contrasting population structure and mtDNA diversity within a marine species flock. Mol Ecol 18:680–696

Jobb G, von Haeseler A, Strimmer K (2004) Treefinder: a powerful graphical analysis environment for molecular phylogenetics. BMC Evol Biol 4:18

Jobb G (2008) TREEFINDER Version October 2008. http://www.treefinder.de/. Accessed August 2010

Jones GP, Milicich MJ, Emslie MJ, Lunow C (1999) Self-recruitment in a coral reef fish population. Nature 402:802–803

Jordan DS (1901) The fish fauna of Japan, with observation on the geographical distribution of fishes. Science, new series vol XIV 354:545–567

Kawabe K (2005) Embryonic development and effect of water temperature on hatching of the Blacktip Grouper, *Epinephelus fasciatus*. Aquaculture Sci 53:333–342

Kawabe K, Kato K, Kimura J (2000) Year round spawning of reared blacktip grouper, *Epinephelus fasciatus*, in Chichi-jima, Ogasawara Islands, southern Japan. Aquaculture Sci 48:467–473

Kawabe K, Kato K, Kimura J, Saito M, Ando K, Kakiuchi K (1997) Growth of reared blacktip grouper *Epinephelus fasciatus* in Chichijima, Ogasawara Islands, Southern Japan. Aquaculture Sci 45:207–212

Kawabe K, Kohno H (2009) Morphological development of larva and juvenile blacktip grouper, *Epinephelus fasciatus*. Fish Sci 75:1239–1251

Kimura M (2000) Paleogeography of the Ryukyu Islands. Tropics 10:5–24

Kimura M (1980) A simple method for estimating evolutionary rates of base substitutions through comparative studies of nucleotide sequences. J Mol Evol 16:111–120

Kimura M, Weiss GH (1964) The stepping stone model of population structure and the decrease of genetic correlation with distance. Genetics 49:561–576

Kuriiwa K, Hanzawa N, Yoshino T, Kimura S, Nishida M (2007) Phylogenetic relationships and natural hybridization in rabbitfishes (Teleostei: Siganidae) inferred from mitochondrial and nuclear DNA analyses. Mol Phylogenet Evol 45:69–80

Liu JX, Gao TX, Wu SF, Zhang YP, (2007) Pleistocene isolation in the Northwestern Pacific marginal seas and limited dispersal in a marine fish, *Chelon haematocheilus* (Temminck and Schlegel, 1845). Mol Ecol 16:275–288

Matsuura K, Senou H (2012) Introduction of Fishes in the Kuroshio Current. In: Matsuura K (ed) Fishes in the Kuroshio Current. Tokai University Press, Kanagawa, pp 3–16

Nakabo T (2002) Characteristics of the fish fauna of Japan and adjacent waters. In: Nakabo T (ed) Fishes of Japan with pictorial keys to the species, English edition. Tokai University Press, Tokyo, pp xliii–lii

Nishimura S (1992) General Remarks. In: Nishimura S (ed) Guide to seashore animals of Japan with color pictures and keys, vol. 1. Hoikusha, Osaka, pp xi–xix

Ota H (1998) Geographic patterns of endemism and speciation in amphibians and reptiles of the Ryukyu Archipelago, Japan, with special reference to their paleogeographical implications. Res Popul Ecol 40:189–204

Palumbi SR (1994) Genetic divergence, reproductive isolation, and marine speciation. Ann Rev Ecol Syst 25:547–572

Rambaut A, Drummond A (2009) TRACER v1.5. http://tree.bio.ed.ac.uk/software/tracer/. Accessed January 2013

Randall JE, Heemstra PC (1991) Revision of Indo-Pacific groupers (Perciformes: Serranidae: Epinephelinae), with descriptions of five new species. Indo-Pacific Fishes No. 20. Bishop Museum, Honolulu, Hawaii

Randall JE, Ida H, Kato K, Pyle RL, Earle JL (1997) Annotated checklist of the inshore fishes of the Ogasawara Islands. Natn Sci Mus Monographs, No. 11. National Science Museum, Tokyo

Rice WR (1989) Analyzing tables of statistical test. Evolution 43:223–225

Riginos C, Nachman MW (2001) Population subdivision in marine environments: the contributions of biogeography, geographical distance and discontinuous habitat to genetic differentiation in a blennioid fish, *Axoclinus nigricaudus*. Mol Ecol 10:1439–1453

Rocha LA, Bass AL, Robertson R, Bowen BW (2002) Adult habitat preferences, larval dispersal, and the comparative phylogeography of three Atlantic surgeonfishes (Teleostei: Acanthuridae). Mol Ecol 11:243–252

Rocha LA, Rocha CR, Robertson DR, Bowen BW (2008) Comparative phylogeography of Atlantic reef fishes indicates both origin and accumulation of diversity in the Caribbean. BMC Evol Biol 8:157

Rogers AR (1995) Genetic evidence for a Pliocene population explosion. Evolution 49:608–615

Rogers AR, Harpending H (1992) Population growth makes waves in the distribution of pairwise genetic differences. Mol Biol Evol 9:552–569

Ronquist F, Teslenko M, Van Der Mark P, Ayres DL, Darling A, Höhna S, Larget B, Liu L, Suchard MA, Huelsenbeck JP (2012) MrBayes 3.2: Efficient Bayesian phylogenetic inference and model choice across a large model space. Syst Biol 61:539–542

Schneider S, Excoffier L (1999) Estimation of past demographic parameters from the distribution of pairwise differences when the mutation rates vary among sites: application to human mitochondrial DNA. Genetics 152:1079–1089

Senou H (2002) Family Serranidae. In: Nakabo T (ed) Fishes of Japan with pictorial keys to the species, English edition. Tokai University Press, Tokyo, pp 690–731

Senou H, Shinohara G, Matsuura K, Furuse K, Kato S, Kikuchi T (2002) Fishes of Hachijo-jima Island, Izu Islands Group, Tokyo, Japan. Mem Nat Sci Mus Tokyo 38:195–237

Senou H, Morita Y, Morishita O (2003) Notes on the distribution of a surgeonfish *Ctenochaetus hawaiiensis* (Perciformes: Acanthuridae). I.O.P. Diving News 14(10):2–4

Senou H, Matsuura K, Shinohara G (2006) Checklist of fishes in the Sagami Sea with zoogeographical comments on shallow water fishes occurring along the coastlines under the influence of the Kuroshio Current. Mem Nat Sci Mus Tokyo 41:389–542

Shimada K (2002) Family Chaetodontidae. In: Nakabo T (ed) Fishes of Japan with pictorial keys to the species, English edition. Tokai University Press, Tokyo, pp 884–897

Shirai S, Kuranaga R, Sugiyama H, Higuchi M (2006) Population structure of the sailfin sandfish, *Arctoscopus japonicas* (Trichondontidae), in the Sea of Japan. Ichthyol Res 53:357–368

Springer VG (1982) Pacific Plate biogeography, with special reference to shorefishes. Smithson Contrib Zool 367. Smithsonian Institution Press, Washington.

Swearer SE, Caselle JE, Lea DW, Warner RR (1999) Larval retention and recruitment in an island population of a coral-reef fish. Nature 402:799–802

Tajima F (1989) Statistical method for testing the neutral mutation hypothesis by DNA polymorphism. Genetics 123:585–595

Tamura K, Nei M (1993) Estimation of the number of nucleotide substitutions in the control region of mitochondrial DNA in humans and chimpanzees. Mol Biol Evol 10:512–526

Tamura K, Peterson D, Stecher G, Nei M, Kumar S (2011) MEGA5: Molecular evolutionary genetics analysis using maximum likelihood, evolutionary distance, and maximum parsimony methods. Mol Biol Evol 28:2731–2739

Tavaré S (1986) Some probabilistic and statistical problems in the analysis of DNA sequences. Lect Mathemat Life Sci (Am Mathemat Soc) 17:57–86

Tanabe AS (2007) KAKUSAN: a computer program to automate the selection of a nucleotide substitution model and the configuration of a mixed model on multilocus data. Mol Ecol Notes 7:962–964

Tanabe AS (2008) Phylogears Version 1.5.2010.03.24. http://www.fifthdimension.jp/. Accessed August 2010

Tanaka S (1931) On the distribution of fishes in Japanese water. J Fac Sci, Imp Univ Tokyo Sec IV Zool 3(1):1–90

Templeton AR, Crandall KA, Sing CF (1992) A cladistic-analysis of phenotypic associations with haplotypes inferred from restriction endonuclease mapping and DNA-sequence data. 3. Cladogram estimation. Genetics 132:619–633

Ujiié H, Ujiié Y (1999) Late Quaternary course changes of the Kuroshio Current in the Ryukyu Arc region, northwestern Pacific Ocean. Mar Micropaleontol 37:23–40

Ujiié Y, Ujiié H, Taira A, Nakamura T, Oguri K (2003) Spatial and temporal variability of surface water in the Kuroshio source region, Pacific Ocean, over the past 21,000 years: evidence from planktonic forminifera. Mar Micropaleontol 49:335–364

Vos RA (2003) Accelerated likelihood surface exploration: the likelihood ratchet. Syst Biol 52:368–373

Yang Z (2007) PAML 4: phylogenetic analysis by maximum likelihood. Mol Biol Evol 24:1586–1591

Yoshigou H (2004) The fishes found from tide-pools and surge sublittral zone in the Minami-daito (South-Borodino) Island, Japan. Misc Rep Hiwa Mus Natl Hist Hiroshima 43:1–51